Catalysis Letters Vol. 112, Nos. 1–2, November 2006 (© 2006)
DOI: 10.1007/s10562-006-0160-5

Catalytic activity of atomized Ni_3Al powder for hydrogen generation by methane steam reforming

Yan Ma,[a,b,]* Ya Xu,[a] Masahiko Demura,[a] Dong Hyun Chun,[a,c] Guoqiang Xie,[d] and Toshiyuki Hirano[a,b]

[a]*National Institute for Materials Science, 1-2-1 Sengen, Tsukuba, Ibaraki, 305-0047, Japan*
[b]*Graduate School of Pure and Applied Sciences, University of Tsukuba, 1-2-1 Sengen, Tsukuba, Ibaraki, 305-0047, Japan*
[c]*Department of Materials Science and Engineering, KAIST, Daejeon, 305-701, Korea*
[d]*Institute for Materials Research, Tohoku University, Katahira 2-1-1, Aoba-Ku, Sendai, 980-8577, Japan*

Received 18 July 2006; accepted 19 September 2006

The catalytic activity of Ni_3Al for methane steam reforming was investigated for the first time using its atomized powder. It was found that the activity was significantly enhanced by the combined pretreatment of acid and alkali leaching, while it was quite low for the as-received powder. The high activity was attributed to the formation of fine Ni particles on the porous surface of the powder.

KEY WORDS: Ni_3Al; atomized powder; catalytic activity; methane steam reforming.

1. Introduction

Hydrogen is mostly produced from natural gas by steam reforming of methane. Methane reacts with steam over a catalyst in the temperature range of 973–1373 K to yield hydrogen, together with carbon dioxide and/or carbon monoxide [1,2]. Much effort has already been made to develop efficient and inexpensive heterogeneous catalysts. Nickel-based catalysts are typical catalysts for this reaction [3]. However, their performance is not satisfactory and more efficient catalysts are required [4].

In Ni–Al system there are four stable compounds, namely $NiAl_3$, Ni_2Al_3, NiAl and Ni_3Al. Among them, a mixture of $NiAl_3$ and Ni_2Al_3 is used as a precursor alloy for Raney nickel catalysts [5,6]. Raney nickel catalysts are produced from this precursor alloy by selectively leaching aluminum in a concentrated NaOH solution. As a result, a porous, high surface-area nickel residue is formed on the surface, which contributes to its high catalytic activity. In contrast, NiAl and Ni_3Al are not used as precursors. It has been thought to be difficult to effectively leach aluminum from them due to their low aluminum concentration, and thus a high catalytic activity has not been expected [7]. Both compounds are well known as excellent high-temperature structural materials with a high-temperature strength and good corrosion/oxidation resistance [8,9].

Recently, our group found that Ni_3Al, both in the form of a powder and foil, exhibits a high catalytic activity for methanol decomposition, leading to hydrogen generation ($CH_3OH \rightarrow 2H_2 + CO$) [10–12]. These results suggest the possibility of a catalytic activity for steam reforming of methane in Ni_3Al.

In the present study, we examined the catalytic activity of Ni_3Al for methane steam reforming using its atomized powder. The effects of chemical pretreatments on the catalytic activity of the powder were investigated.

2. Experimental

A stoichiometric Ni_3Al (Ni–25 at.% Al) powder was obtained from Kojunndo Chemical Lab. Co. Ltd., Japan. It was prepared by a gas atomizing process and sieved for less than 150 in. size. The as-received powder was chemically pretreated in the following four ways before the catalytic experiments as listed in table 1. Processes (a) and (b) are single-step treatments. Process (a) is a dip treatment at 366 K for 300 min in a stirred 20 wt% aqueous NaOH solution (alkali leaching), and process (b) is the one at 298 K for 15 min in 2 vol.% aqueous HNO_3 (acid leaching). Processes (c) and (d) are two-step treatments in combination with processes (a) and (b). Process (c) is the treatment using process (b) followed by process (a), and process (d) is that of the reverse order. After each step of the pretreatments, the solution was subjected to an inductively coupled plasma (ICP) analysis in order to measure the amounts of aluminum and nickel leached from the powder. After rinsing in deionized water and dring at 323 K for 8 h, the surface area of the powder was determined by the Brunauer–Emmett–Teller (BET) surface area analysis method using krypton adsorption (Micromeritics, ASAP 2020). The surface morphologies of the powder

---

*To whom correspondence should be addressed.
E-mail: MA.Yan@nims.go.jp

Table 1
Results of ICP and BET surface area

Pretreatment process		ICP results – amount of leached elements (wt%)		BET surface area ($m^2\ g^{-1}$)
		Al	Ni	
(a)	In 20 wt% NaOH, at 366 K, for 300 min	2.41	BDL	0.06
(b)	In 2 vol.% HNO_3, at 298 K for 15 min	7.86	7.66	0.12
(c)	Step 1: in 2 vol.% HNO_3 at 298 K for 15 min	7.86	7.66	0.41
	Step 2: in 20 wt% NaOH at 366 K for 300 min	3.47	BDL	
	Total	11.33	7.66	
(d)	Step 1: in 20 wt% NaOH at 366 K for 300 min	2.41	BDL	0.23
	Step 2: in 2 vol.% HNO_3 at 298 K for 15 min	11.76	12.32	
	Total	14.17	12.32	

BDL signifies below detection limit.

were observed by scanning electron microscopy (SEM: JEOL, JSM-7000F). The surface structure and composition were determined by transmission electron microscopy (TEM: JEOL, JSM-2100F) coupled with an X-ray energy dispersive spectroscopy (EDS) system. The crystal structure before and after the pretreatments were analyzed by X-ray diffraction (XRD) using a Cu Kα source (Rigaku, RINT2500).

The catalytic experiments were carried out in a conventional fixed-bed flow reactor in the same way as described in previous reports [10–12]. A 0.4 g sample of Ni_3Al powder was placed in a quartz tube with an internal diameter of 8 mm and then into the stove. Prior to the reaction, the powder was reduced at 873 K for 1 h in a flowing hydrogen atmosphere. The hydrogen flow was then stopped and filled with pure nitrogen to flush the hydrogen. Subsequently, mixed reactants of CH_4 and H_2O (mole ratio of $H_2O/CH_4 = 3$) were introduced into the quartz tube reactor at the gas hourly space velocity (GHSV) of 12,000 h^{-1} (defined as the volume of CH_4 passed over the unit volume of catalyst per hour). The H_2O was fully evaporated in a thermal evaporator before introducing it into the reactor. Finally, the temperature was stepwise increased from 873 to 1173 K at intervals of 50 K. The composition of the outlet gas products was analyzed after a lapse of 30 min at each temperature using a gas chromatograph (GL Science, GC-323 equipped with thermal conductivity detectors). The total flow rate of the gas products was measured at each temperature using a soap bubble meter just after the gas analysis.

3. Results

3.1. As-received powder

The as-received powder has the overall stoichiometric composition of Ni_3Al. However, since it was rapidly solidified during the atomizing process, it has a second phase in the Ni_3Al matrix (shown as dark strip in figure 1(a)). The second phase is mostly lamellar (100–200 nm thick) and partly dendritic. An EDS

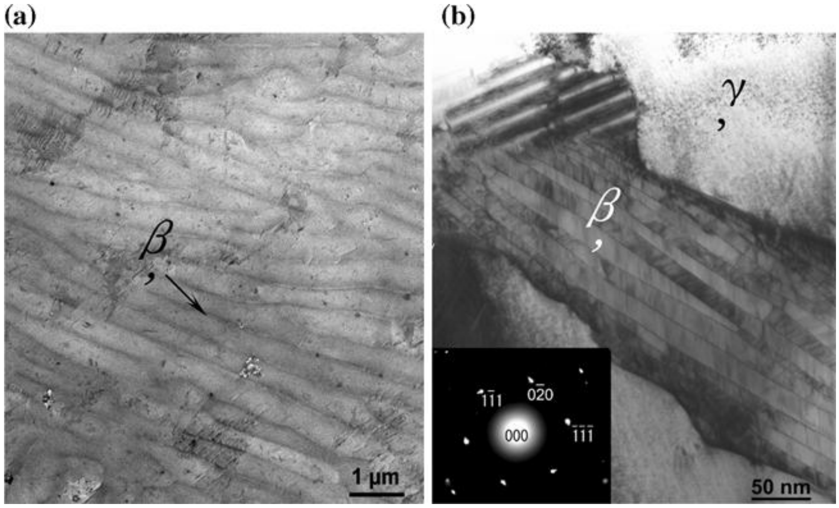

Figure 1. (a) SEM image of as-received atomized Ni_3Al powder and (b) TEM bright field image showing the second phase with lamellar structure. The inset is the corresponding selected area diffraction patterns from the lamellar phase, showing $L1_0$–type β'-NiAl.

analysis indicated that the second phase is enriched in aluminum compared to the Ni_3Al matrix. Figure 1(b), the TEM bright field image, shows that the second phase consists of a lamellar structure with many planar faults. The inset is the corresponding selected-area diffraction pattern obtained from the lamellar phase. The pattern was identified as $L1_0$–type β'-NiAl, which agrees with the result observed on the rapidly solidified Ni_3Al powder by Baker *et al.* [13,14]. The formation process of β'-NiAl was proposed by Baker *et al.* [14].

3.2. Characterization of chemically pretreated powder

Table 1 summarizes the ICP analysis results of the pretreated solutions. The amounts of leached aluminum and nickel are shown by the percentage to the chemical composition of the as-received powder. In process (a), a small amount of aluminum was selectively leached out by the NaOH solution, indicating that the surface was enriched in nickel after the treatment. In process (b), aluminum and nickel were almost equally leached into the HNO_3 solution. The surface composition probably remained unchanged. In the two-step treatment, more elements were leached in the second step than in the corresponding single step. In process (c), the amount of leached aluminum in the second step is 1.4 times greater than that in process (a), indicating that the surface became more enriched in nickel than in process (a). In process (d), the amount of leached aluminum and nickel in the second step was 1.7 times greater than that in process (b). The surface became enriched in nickel after the first step, but it was considered to be spoiled after the second step. Basically, the surface became enriched in nickel after process (a) and (c), probably more after process (c), while a compositional change in the surface was small after processes (b) and (d).

The surface areas measured by the BET method are also listed in table 1. The surface area of the powder treated by process (a) is very low and almost the same as that of the as-received powder. The surface area increased using processes (c) and (d). These results indicate that the combination process effectively enhances the surface area, though the surface area is still low compared to that of common catalysts.

The SEM images in figure 2 show the surface morphology of the pretreated powder. In the powder treated by process (a), a morphological change is slightly observed both in the β'-NiAl and Ni_3Al (figure 2(a)). There is probably a very small difference in the selective aluminum leaching between the two phases. In the powder treated by process (b), the β'-NiAl preferentially dissolved in the HNO_3 solution over the Ni_3Al matrix, leaving a lamellar porous structure on the surface (figure 2(b)). The lamellar pore is macroscopic in size and in the range of 100–500 nm in width. The preferential dissolution of β'-NiAl is reasonable from the fact that β'-NiAl is more easily etched by an acid solution than Ni_3Al [14]. Compared to the single-step treatments, the two-step treatments, processes (c) and (d), left more complicated and porous surface (figure 2(c) and (d)).

The powders were examined by XRD after the chemical pretreatments. All the diffraction peaks were assigned as $L1_2$–type γ'-Ni_3Al whether untreated or pretreated. Aluminum was selectively leached from the surface in processes (a) and (c), but no Ni was detected. It is considered that the selective aluminum leaching is

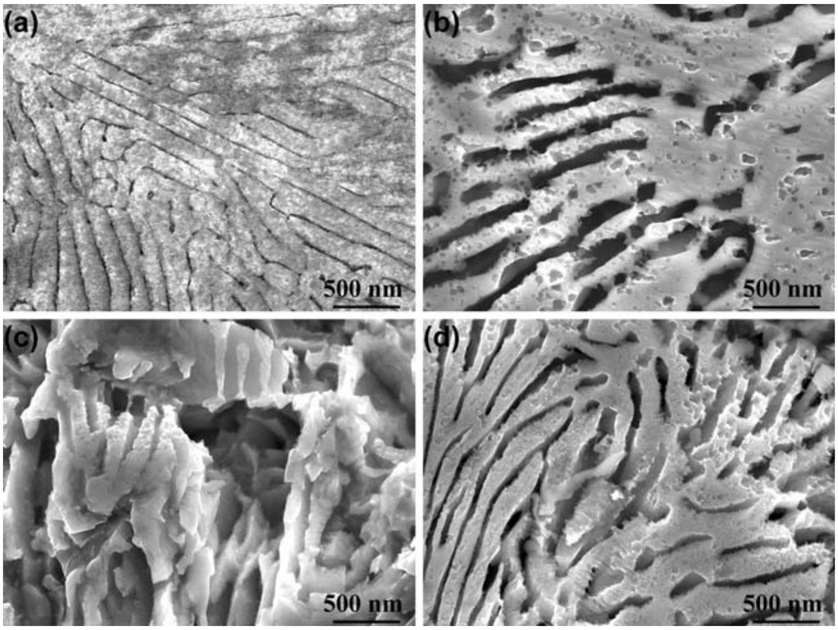

Figure 2. SEM images of (a) alkali leached, (b) acid leached, (c) acid + alkali leached, and (d) alkali + acid leached powders.

limited to the thin surface layer of the powder, leaving the bulk as is. No β'-NiAl ($L1_0$–type) was also detected, probably due to peak broadening by the strain generated during the rapid solidification.

3.3. Catalytic activity

The catalytic activity was isochronally measured under the conditions of pressure = 1.013 bar and S/C = 3 from 873 to 1223 K. Three gaseous products, H_2, CO, and CO_2, were detected at the reactor outlet by gas chromatography. Figure 3 plots the production rates of H_2, CO, and CO_2 as a function of the reaction temperature.

There are noteworthy features in hydrogen production (figure 3(a)). First, hydrogen is produced at high temperatures over all the powders and even over the untreated as-received one, indicating that the atomized Ni_3Al powder has some catalytic activity for methane steam reforming. Second, process (c) significantly reduces the onset temperature of the catalytic activity. The onset temperature of the as-received powder is higher than 1173 K, and it is not affected by processes (a) and (b). In contrast, the effect of process (c) is remarkable. The onset temperature was reduced to less than 873 K. Another two-step pretreatment, process (d), tends to reduce the onset temperature, but the effect was less. Third is the temperature dependence of the production rate of H_2 in the powder treated by process (c). It increased with the increasing temperature up to 1073 K and then reached a steady state of 145 mL min^{-1} (STP).

Carbon monoxide and carbon dioxide are also effectively produced in the powder treated by process (c) (figure 3(b) and (c)). However, the temperature dependence of their production rates is different from each other and that of hydrogen. The production rate of CO monotonously increased with the increasing temperature, while that of CO_2 slightly increased with the temperature between 873 and 923 K, and then gradually decreases at temperatures above 973 K, showing a broad peak around 923 K.

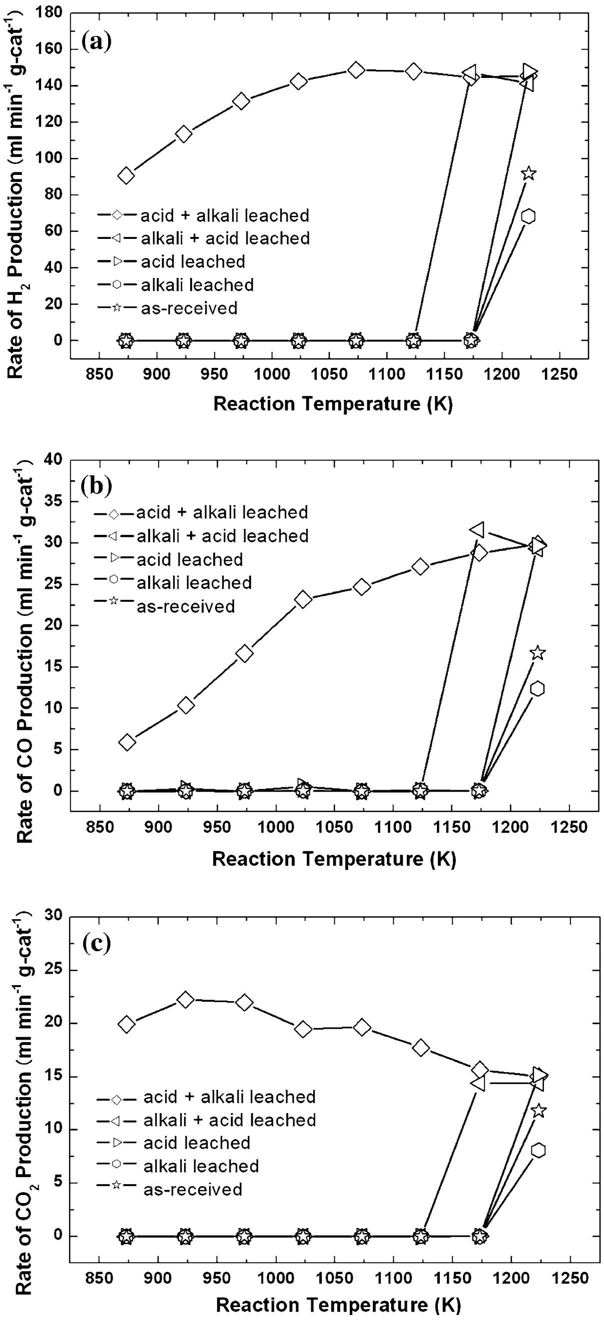

Figure 3. Rate of (a) H_2, (b) CO, and (c) CO_2 production during methane steam reforming over pretreated and as-received Ni_3Al powders as a function of reaction temperature.

4. Discussion

4.1. *Effect of pretreatments on the catalytic activity*

It was pointed out in Section 3.3 that atomized Ni_3Al powder has a catalytic activity at high temperatures for methane steam reforming, and the onset temperature is significantly reduced by a consecutive combination of acid and alkali leaching, process (c), among the four pretreatments. We will now discuss the effect of the pretreatment on the catalytic activity.

The results in Section 3.2 (table 1, figure 2) revealed that the powder surface varies depending on the pretreatments. The surface became Ni-enriched after process (a), porous after process (b), porous and Ni-enriched after process (c) and porous, but not Ni-enriched after process (d). We consider that having a porous and Ni-enriched surface is the major reason for reducing the onset temperature of the catalytic reaction. This surface state is achieved only by process (c), and not by the other three pretreatments.

As described in Section3.1, the as-received atomized powder contained β'-NiAl in the Ni_3Al matrix because it was produced by rapid solidification. Obviously, the

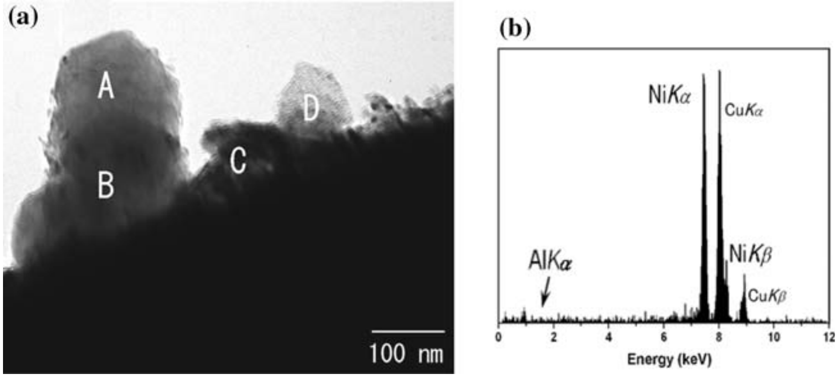

Figure 4. (a) TEM bright field image of the powder treated by process (c), showing the formation of fine particles on the surface, and (b) EDS spectra taken from position B showing that the particles are composed of pure Ni (TEM sample was supported on a copper mesh).

presence of the lamellar β′-NiAl contributed to the formation of the porous surface. β′-NiAl was preferentially dissolved in the HNO_3 solution over the Ni_3Al matrix, leaving a lamellar porous structure on the surface (figure 2(b)), and as a result, the BET surface area increased (table 1). In process (c), the following alkali leaching changed the porous surface into a Ni-enriched one (table 1), resulting in the significant reduction of the onset temperature.

A TEM analysis was carried out on the powder treated by process (c) in order to investigate the surface structure in more detail. Figure 4(a) shows the bright field image. It is noted that many fine particles are present on the surface. The EDS spectra were taken at positions A, B, C and D in figure 4(a). All the spectra were quite similar. Figure 4(b) shows the spectra taken at position B. The EDS analysis revealed that the particles are composed of almost pure Ni. An aluminum peak was hardly detected. The copper spectra in the figure are the reflection from the specimen support. Therefore, the results confirmed that plenty of fine Ni particles are produced during process (c). As is well known, fine Ni particles are catalytically active for methane steam reforming [15].

4.2. Catalytic behavior

We will now discuss the catalytic behavior for the powder treated by process (c) in figure 3. We assume that the following two chemical reversible reactions are involved under excess steam (S/C = 3) conditions:

$$CH_4 + H_2O \Leftrightarrow 3H_2 + CO \quad \Delta H = +206\,\text{kJ/mol} \qquad (1)$$

$$CO + H_2O \Leftrightarrow H_2 + CO_2\Delta \quad H = -41\,\text{kJ/ mol} \qquad (2)$$

This assumption is valid because carbon maintains a balance between the inlet for CH_4 and outlet for the mixed CO, CO_2, and CH_4, and the molecule number of H_2, CO, and CO_2 holds stoichiometric relation in equation (1) and (2). Other side reactions can then be ignored. As is well known, the methane steam reforming reaction (1) is strongly endothermic and thermodynamically favored by high temperatures, while the water-gas shift reaction (2) is moderately exothermic and favored by low temperatures [16–18].

Figure 5(a) shows the conversions of methane and steam. The methane conversion rapidly increases with the increasing temperature up to 1073 K, consistent with

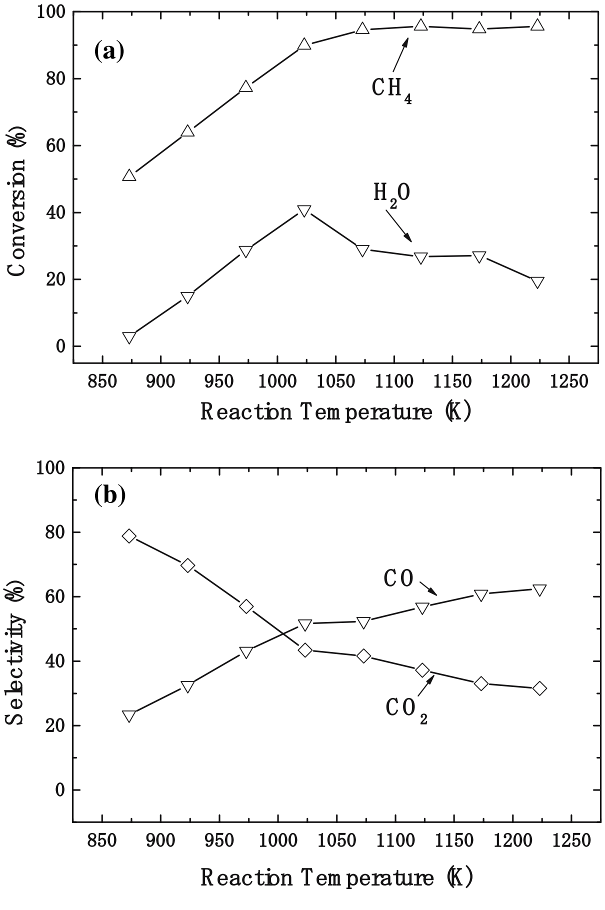

Figure 5. (a) Conversions of CH_4 and H_2O and (b) selectivities of CO and CO_2 for methane steam reforming over the powder treated by process (c) as a function of reaction temperature.

its endothermic reaction. Above 1073 K it reaches a steady-state with a value of about 95%, which means that almost all amounts of the feed methane are converted to H_2 and CO via the forward reaction of (1). Namely, the powder treated by process (c) is quite catalytically active in this temperature range. Steam conversion shows the same temperature tendency as the methane conversion below 1023 K, while it decreases at temperatures above1023 K, indicating that the forward reaction of (2) occurred less and less with temperature. Figure 5(b) shows the selectivities of CO and CO_2, which are calculated as (molecules of CO/molecules of CH_4 converted) × 100 and (molecules of CO_2/molecules of CH_4 converted) × 100, respectively. With the increasing reaction temperature, the selectivity of CO increases, while that of CO_2 decreases. Since CO_2 is the product of the chain reactions of (1) and (2), the selectivity of CO_2 expresses the degree of reaction (2) under an excess steam condition, i.e., conversion of CO to CO_2. Thus the small negative temperature dependency of CO_2 is attributed to its moderate exothermic reaction. Due to this negative temperature dependency, reaction (2) occurred less at high temperatures, leading to the increased selectivity of CO.

It was concluded that the catalytic behavior of the atomized powder treated by process (c) was reasonably understood by assuming methane steam reforming and water–gas shift reaction.

5. Conclusions

The catalytic activities of atomized Ni_3Al powder for methane steam reforming were investigated in the temperature range of 873–1223 K, and the effects of chemical pretreatments were evaluated. The following results were obtained. These results demonstrate that Ni_3Al powder can serve as catalyst precursors for hydrogen generation by methane steam reforming.

(1) The as-received atomized Ni_3Al powder exhibited a catalytic activity above 1173 K.
(2) The catalytic activity was improved by the consecutive combination of acid and alkali leaching (process (c)). The onset temperature of the catalytic activity was reduced to less than 873 K.
(3) The reason of the high activity was attributed to the formation of fine Ni particles on the porous surface by process (c).
(4) The catalytic behavior was understood by assuming methane steam reforming and water–gas shift reaction.

References

[1] J.N. Armor, Catal. Lett. 101 (2005) 131.
[2] G.W. Crabtree, M.S. Dresselhaus and M.V. Buchanan, Phys. Today 57(12) (2004) 39.
[3] J.R. Rostrup-Nielsen, in: *Catalysis, Science and Technology*, Vol. 5, eds. J.R. Anderson and M. Boudart (Springer, Berlin, 1984) ch. 1.
[4] J.R. Rostrup-Nielsen, J. Sehested and J.K. Nørskov, Adv. Catal. 47 (2002) 65.
[5] M.S. Wainwright, *Preparation of Solid Catalysts* (Wiley-Vch, New York, 1999).
[6] M. Raney. US Patent 162,810 (1927).
[7] S. Tanaka, N. Hirose, T. Tanaki and Y.H. Ogata, J. Electrochem. Soc. 147 (2000) 2242.
[8] C.T. Liu and D.P. Pope, in: *Intermetallic Compounds – Practice*, J.H. Westbrook and R.L Fleischer (eds.), Vol. 2 (Wiley, Chichester, 1995) pp. 17–51.
[9] D.B. Miracle and R. Darolia, in: *Intermetallic Compounds – Practice*, J.H. Westbrook and R.L. Fleischer (eds.), Vol. 2 (Wiley, Chichester, 1995) pp. 53–72.
[10] Y. Xu, S. Kameoka, K. Kishida, M. Demura, A. Tsai and T. Hirano, Mater. Trans. 45 (2004) 3177.
[11] Y. Xu, S. Kameoka, M. Demura, A. Tsai and T. Hirano, Intermetallics 13 (2005) 151.
[12] D.H. Chun, Y. Xu, M. Demura, K. Kishida, M.H. Oh, T. Hirano and D.M. Wee, Catal. Lett. 106 (2006) 71.
[13] I. Baker, F.S. Ichishita, V.A. Surprenant and E.M. Schulson, Metallography 17 (1984) 299.
[14] I. Baker, J.A. Horton and E.M. Schulson, Metallography 19 (1986) 63.
[15] H.S. Bengaard, J.K. Nørskov, J. Sehested, B.S. Clausenb, L.P. Nielsen, A.M. Molenbroek and J.R. Rostrup-Nielsen, J. Catal. 209 (2002) 365.
[16] L.F. Brown, Int. J. Hydrogen Energy 26 (2001) 384.
[17] J. X and G.F. Froment, AICHE J. 35(1) (1989) 88.
[18] M.A. Soliman, A.M. Adris, A.S. Al-Ubaid and S.S.E.H. El-Nashaie, J. Chem. Tech. Biotechnol. 55 (1992) 131.